Geometries and materials for subwavelength surface plasmon modes

Rashid Zia, Mark D. Selker, Peter B. Catrysse, and Mark L. Brongersma

Geballe Laboratory for Advanced Materials, Stanford University, Stanford, California 94305

Received May 18, 2004; revised manuscript received July 21, 2004; accepted July 29, 2004

Plasmonic waveguides can guide light along metal–dielectric interfaces with propagating wave vectors of greater magnitude than are available in free space and hence with propagating wavelengths shorter than those in vacuum. This is a necessary, rather than sufficient, condition for subwavelength confinement of the optical mode. By use of the reflection pole method, the two-dimensional modal solutions for single planar waveguides as well as adjacent waveguide systems are solved. We demonstrate that, to achieve subwavelength pitches, a metal–insulator–metal geometry is required with higher confinement factors and smaller spatial extent than conventional insulator–metal–insulator structures. The resulting trade-off between propagation and confinement for surface plasmons is discussed, and optimization by materials selection is described.

OCIS codes: 130.2790, 160.3900, 240.0310, 240.5420, 240.6680, 260.2110.

1. INTRODUCTION

Surface plasmon–polaritons (SPPs) have received much attention in recent years for their ability to guide electromagnetic energy at optical frequencies.[1] As opposed to dielectric waveguides, wherein light is confined in an optically dense core via index contrast with a cladding region ($\varepsilon_{\text{clad}} < \varepsilon_{\text{core}}$), plasmonic waveguides confine light to metal–dielectric interfaces owing to the negative dielectric constant of the metallic region ($\Re\{\varepsilon_{\text{metal}}\} < 0 < \varepsilon_{\text{dielectric}}$). This surface localization has led researchers to explore the potential to guide SPPs along structures with physical dimensions much smaller than those possible with dielectric waveguides.[2–5] Initial experimental results for metallic wires, particle arrays, and stripes have demonstrated the guiding nature of each of these structures.[6–8] However, a significant drawback to practical use of SPPs for subwavelength confinement results from resistive heating losses in the metal, and the longest measured propagation length for a structure with subwavelength features in two dimensions has been 2.5 μm.[8]

For structures in which subwavelength confinement in one dimension, rather than two dimensions, is required, it has been shown that thin metal films of finite width can be used to propagate electromagnetic energy over several millimeters.[9] Such waveguides possess field-symmetric modal solutions very similar in nature to the long-range SPP modes found in infinite metal films, whereby a coupling of surface plasmons at two metal–dielectric interfaces results in a very small field concentration within the metallic center.[10–12] The effect of this coupling is to reduce the losses resulting from interaction with the metal but likewise to reduce confinement in both lateral and vertical dimensions.[13,14] Although this trade-off has been explicitly stated, no practical expression of the limits of such geometries has been described, nor has the practical pitch of generalized plasmonic structures been derived. In the following, we will investigate the conditions required for subwavelength confinement of metallic slab waveguides. Owing to considerable experimental interest, we will consider only the transverse field-symmetric modes that have been proposed as long-range plasmonic waveguides and are easily coupled to by end-fire excitation.[9] Comparing the numerical solutions for the modes of individual plasmonic waveguides with those of arrayed systems, we will explore the applicability of dielectric waveguide concepts such as spatial extent and confinement factors and demonstrate the precise trade-off posed by propagation and confinement. Given this limitation, the effects of geometry and material selection are investigated.

2. SUBWAVELENGTH CONFINEMENT AND GEOMETRY

The minimum confinement of a guided optical mode is ultimately limited by the Heisenberg uncertainty principle, and derivations of the minimum mode size ($\lambda/2n$) in a conventional dielectric waveguide have been presented previously.[2] Although uncertainty must again limit the confinement in a plasmonic waveguide, the expansion of the aforementioned derivations to describe modes of purely evanescent fields is nontrivial. Such analysis would require the validation of a wave-vector basis set describing the evanescent waves at each interface, as well as a minimization of this set's representation (i.e., spatial extent) in real space.

Fortunately, the same surface wave nature that complicates uncertainty analyses also suggests the relevance of more intuitive decay length calculations. Consider the isotropic wave equation for a generic three-layer plasmonic slab waveguide with metallic and dielectric regions,

$$k_{x,\mathrm{metal}}^2 + k_{y,\mathrm{metal}}^2 + k_z^2 = \frac{\omega^2}{c^2}\varepsilon_{\mathrm{metal}},$$

$$k_{x,\mathrm{dielec}}^2 + k_{y,\mathrm{dielec}}^2 + k_z^2 = \frac{\omega^2}{c^2}\varepsilon_{\mathrm{dielec}}, \quad (1)$$

where z is the propagation direction and thus k_z is the conserved quantity. For a guided surface-plasmon mode to exist,

$$k_z \geqslant \frac{\omega}{c}\sqrt{\varepsilon_{\mathrm{dielec}}}. \quad (2)$$

Thus, if the radiation is unconfined in the y dimension (i.e., $k_y = 0$), the evanescent decay of the fields can be described by the following transverse wave vectors:

$$k_{x,\mathrm{metal}} = i\left(k_z^2 - \frac{\omega^2}{c^2}\varepsilon_{\mathrm{metal}}\right)^{1/2},$$

$$k_{x,\mathrm{dielec}} = i\left(k_z^2 - \frac{\omega^2}{c^2}\varepsilon_{\mathrm{dielec}}\right)^{1/2}. \quad (3)$$

If the spatial extent of the fields is considered one measure of confinement, the ultimate confinement of a thin metal film plasmonic waveguide (e.g., Fig. 1, left-hand side) will be limited by the decay length into the dielectric cladding. Hence, for confinement below the limit of a conventional dielectric waveguide ($\lambda/2n$), a minimum limit is placed on the propagating wave vector:

$$|k_{x,\mathrm{dielec}}| \geqslant \frac{2\pi n_{\mathrm{dielec}}}{\lambda} = \frac{\omega}{c}\sqrt{\varepsilon_{\mathrm{dielec}}},$$

$$\therefore k_z \geqslant \frac{\omega}{c}\sqrt{2\varepsilon_{\mathrm{dielec}}}. \quad (4)$$

Note that this condition is met only near the surface-plasmon resonance frequency. For the majority of frequencies below this resonance, the surface-plasmon dispersion relationship remains near the light line for the dielectric material. This implies that the confinement of such a plasmonic waveguide would be far from subwavelength because the field extent into the surrounding dielectric regions would have a very long decay length.

The relationship represented by Eqs. (3) suggests another plasmonic waveguide for subwavelength confinement, one with metallic cladding layers and a dielectric core as shown schematically in the right part of Fig. 1. Such an MIM waveguide has been considered before and was proposed long ago as a highly tunable waveguide.[15,16] Recent work has begun to highlight potential applications for the MIM structure,[17–19] and it is presented here as an alternative to the low confinement of IMI plasmonic waveguides. The confinement of the MIM structure is limited by the decay length into the metallic regions, which can be approximated as follows for metals below the surface-plasmon resonance:

$$\Re\{\varepsilon_{\mathrm{metal}}\} < -\varepsilon_{\mathrm{dielec}},$$

$$\therefore |k_{x,\mathrm{metal}}| > \frac{\omega}{c}\sqrt{2\varepsilon_{\mathrm{dielec}}} > \frac{2\pi n_{\mathrm{dielec}}}{\lambda}. \quad (5)$$

This improved confinement is a product of increased field intensities within the lossy metallic regions as compared with an IMI structure, and therefore there must be a clear trade-off between propagation length and confinement.

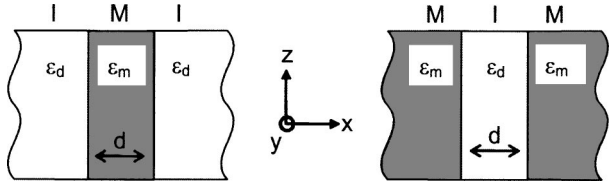

Fig. 1. Insulator–metal–insulator (IMI) (left) and metal–insulator–metal (MIM) (right) geometries for plasmonic slab waveguides with center layer thickness d.

3. ANALYSIS OF INDIVIDUAL MODAL SOLUTIONS

The most intuitive way to quantify the trade-off between propagation length and confinement is by a set of descriptors based directly on the modal solutions of individual plasmonic waveguides; these descriptors, propagation length, beam diameter, and confinement factor are now defined (see insets in Fig. 2 below). For propagation length, the well-established quantifier is the distance wherein the electric field intensity of a traveling wave at either surface decays by a factor of $1/e$. In the literature, two separate parameters have been adapted from dielectric optics to describe the confinement of metallic waveguides. The first term, beam diameter (D_H), describes the spatial extent of the propagating mode by the distance between the points in the two cladding regions where the magnetic field decays to $1/e$ of its peak value.[2] The second term, confinement factor (Γ), represents the ratio of power in the center region of the waveguide to the total power in the waveguide.[14] As we will consider only field-symmetric TM modes, the confinement factor can be defined as follows:

$$\Gamma = \frac{\int_{\mathrm{cent\ lay}} |E_x H_y^*| \mathrm{d}x}{\int_{-\infty}^{+\infty} |E_x H_y^*| \mathrm{d}x}. \quad (6)$$

Determining the precise modal solutions of a multilayered metallic waveguide involves finding the complex roots to the dispersion relationship, a transcendental equation. Although it is possible to use various rudimentary numerical algorithms for this purpose, several techniques have been developed to specifically solve this problem with high numerical accuracy.[20–22] For this study, we have implemented the reflection pole method described in Ref. 21. The technique, based on the transfer-matrix formalism, monitors the phase of the reflection coefficient denominator and can be used to solve for the complex propagation constants of both bound and leaky modes in lossy waveguides. For validation, our implementation was tested against the published solutions of both lossless and lossy dielectric waveguides, antireso-

nant reflecting optical waveguides, and leaky waveguides in addition to plasmonic waveguides composed of single metal–dielectric interfaces, thin metal films bound by the same dielectric, and air–metal–dielectric slabs in the Kretschmann geometry.[20,22] The solutions for the real (β) and imaginary (α) components of the normalized propagation constant were found to be accurate to 10^{-6} and 10^{-8}, respectively.

Next, the modal solutions of Au–air plasmonic waveguides were calculated for a free-space excitation wavelength of 1.55 μm ($\varepsilon_{Au} = -95.92 + i10.97$).[23] Figure 2 shows the propagation lengths, spatial extents, and confinement factors for both IMI and MIM waveguides as a function of center layer thickness (d). For thick waveguides, the propagation lengths for both geometries approach that of a single Au–air interface. However, as the center layer thickness decreases and the SPPs at the two interfaces couple, the propagation length along MIM structures decreases, whereas it increases along IMI structures. It is important to note that the departure from the single-interface solution occurs at around 12.5 μm for the MIM as compared with 100 nm for the IMI. This 2-order-of-magnitude difference demonstrates that the SPP fields decay much more rapidly in the metallic center of the IMI, as expected. Although the spatial extent for both geometries initially decreases with center layer thickness for thick waveguides, as soon as the IMI mode splits from the single-interface solution, the fields of the SPP are pushed into the surrounding dielectric materials, and the spatial extent increases dramatically. Therefore only for the MIM case does the spatial extent decrease to subwavelength levels [$\sim$100 nm $<$ (λ/15) for d = 50 nm], the minimum spatial extent for the IMI case being $\sim$5 μm (i.e., $>3\lambda$). Moreover, the confinement factor for the MIM geometries is 4 orders of magnitude greater than that of IMIs. Despite a slight rise in confinement as the two interfaces couple in the IMI around 100 nm, only a tiny fraction ($<$0.02%) of the optical mode is contained within the center region, whereas practically the entire optical mode is so contained for the MIM. Thus the additional spatial extent of the IMI accounts for nearly the complete optical mode.

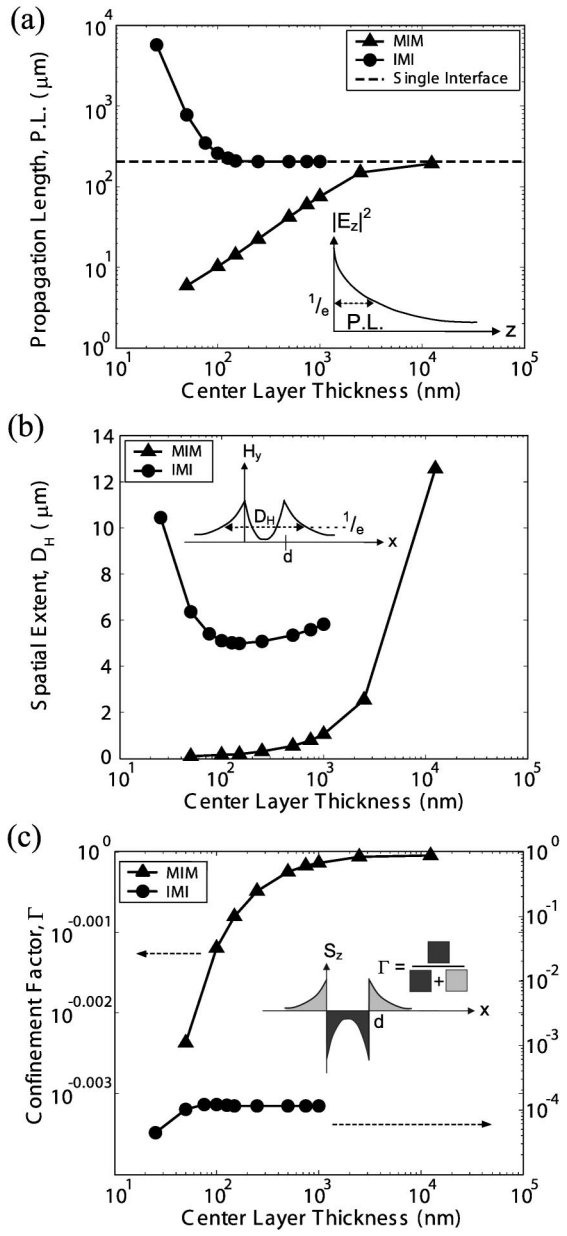

Fig. 2. Description of MIM and IMI plasmonic waveguides (Au–air, λ = 1.55 μm) as a function of decreasing center layer thickness by (a) propagation length, (b) spatial extent, and (c) confinement factor. Insets graphically illustrate plotted terms. (Markers denote the exact location of simulated data points.)

Although IMI geometries provide for longer propagation lengths than achievable along a single interface, the cost is a severe decrease in confinement as the SPP fields are pushed out of the central metallic region into the surrounding dielectric. If plasmonic waveguides are intended to propagate light in subwavelength modes, MIM geometries with higher confinement factors and shorter spatial extents are much better suited for this purpose. Specifically, if plasmonic waveguides are to be used as signal transmission lines for nanophotonics, it is important to consider the achievable packing densities.

4. PITCH AND PROPAGATION FACTORS IN SYSTEMS

For two-dimensional waveguides, the relevant packing density can be expressed in terms of the minimum center-to-center pitch between adjacent waveguides. Although waveguides separated by large distances can transmit SPP signals without interference, waveguides placed in close proximity encounter signal distortion due to coupling losses between waveguides as well as perturbations of the waveguide modes. We will call these two effects mode coupling and mode splitting. Often for dielectric waveguides, mode coupling (i.e., cross talk) places a limit on device pitches far before mode splitting is significant. However, the limitations on cross talk are generally application specific because they depend on the relevant signals and detectors in a complete communication architecture. Given the nascent state of plasmonic devices, a minimum pitch based on mode splitting would provide a more fundamental limit. When the modes of two adjacent waves begin to overlap to such an extent that the solutions of both are significantly perturbed, the signal is no

longer localized on a single waveguide, and thus a pitch calculation based on mode splitting would represent the absolute limit of device densities.

To simulate a two-waveguide system, we used the reflection pole method to calculate the modes of five-layered insulator–metal–insulator–metal–insulator (IMIMI) and metal–insulator–metal–insulator–metal (MIMIM) systems to simulate adjacent IMI and MIM waveguides, respectively. In the reflection pole method the initial splitting of two formerly degenerate modes can be monitored by assuming that only one mode exists. As the modes split, the calculated imaginary component of the propagation constant (α) increases. To ensure that our analysis was not biased with respect to our hypothesis, we set more stringent conditions for confinement in the MIM geometry. For the IMI and single-interface cases, the minimum pitch was determined by the smallest value of the shared cladding thickness for which the imaginary propagation constant remained unchanged to the 10^{-6} term as compared with the degenerate case. For the MIM geometry, a change in the 10^{-8} term was used to determine pitch. Considering the relative magnitude of the imaginary propagation constant in both structures, this is a significantly more rigorous condition (roughly a 0.01% change for MIMs as opposed to a 10% change for IMIs). For each of the core thicknesses (d) previously considered for the individual waveguides, the thickness of the shared cladding region was varied by 25-nm steps to determine the pitch. Thus, for the IMI case, the thickness of the center insulator layer within the IMIMI was decreased until significant mode splitting began.

In Fig. 3 the propagation length of both IMI and MIM waveguides are plotted as a function of these calculated pitches. In addition to Au–air waveguides, Cu–air and Al–air waveguides have been considered at 1.55 μm ($\varepsilon_{Cu} = -67.86 + i10.01$, $\varepsilon_{Al} = -252.5 + i46.07$).[23] As classified by pitch and propagation length, the two geometries clearly occupy two opposite quadrants when compared with the single-interface case. The IMI geometry offers longer propagation for larger pitches, whereas the MIM geometry provides for tighter pitches at the expense of reduced propagation lengths. For example, if one requires plasmonic waveguides with a sub-12-μm pitch, only an MIM-based system could be used, and the maximum propagation length would be less than 200 μm. However, if a propagation length of 300 μm was necessary, this could be achieved with IMI-based waveguides spaced at a pitch greater than 30 μm. Thus the geometric trade-off can be defined for a particular wavelength by solving for the propagation length and pitch of a single interface.

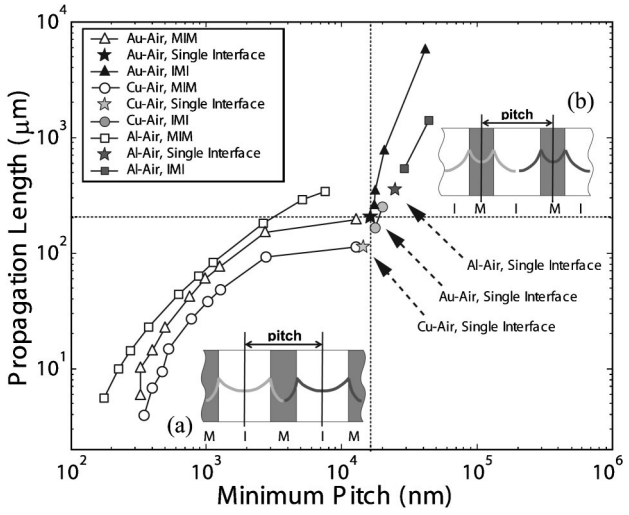

Fig. 3. Trade-off between propagation length and minimum pitch for plasmonic waveguides of various materials at 1.55 μm. Dotted lines highlight the propagation length and achievable pitch of single-interface Au–air waveguides. Insets depict the modal distributions and pitch definitions for (a) MIM and (b) IMI geometries. (Markers denote the exact location of simulated data points.)

Having defined the geometric limitations, though, we find that the logical goal becomes the design of a waveguide with both tighter pitches and longer propagation lengths than the single-interface case. How does one access the desirable upper left quadrant in the pitch–propagation plot? One idea would be to increase frequency (which generally lowers heating losses in the metal, shifting the plots upward), yet this is often impractical in a real architecture given a specific source and detector setup. The other obvious choice would be to vary the materials used. Unfortunately, for initial calculations based on air as the dielectric, the sole option is to increase the optical density of the dielectric, which would have a detrimental effect on pitch (i.e., the plot would shift rightward). The only practical choice is thus to vary the metal used in the waveguide. Although the precise effect of such a variation is difficult to predict given the change in both real and imaginary components of the complex dielectric function, the pitch–propagation plot allows for a simple comparison of the result. For example, at 1.55 μm, Cu has worse characteristics when compared with Au, whereas Al can achieve shorter pitches for longer propagation lengths than either Au or Cu. Therefore, if one needed a plasmonic waveguide to meet both earlier requirements (i.e., 300-μm propagation length and sub-20-μm pitch), an Al-based MIM structure would be the appropriate choice. Or, of greater interest, if one needed a 50-μm propagation length for waveguides at a sub-700-nm pitch, Al-based MIM structures would also be the appropriate choice.

5. CONCLUSIONS FOR SUBWAVELENGTH PLASMONIC WAVEGUIDES

Accordingly, for plasmonic waveguides to truly fulfill their promise as subwavelength waveguides, specific geometries must be chosen to optimize confinement. For the field-symmetric planar case, we have demonstrated that this would require an MIM structure. Additionally, we have defined the cost of this confinement in terms of shorter propagation length, offered a metric on which to compare various structures, and presented options in terms of both wavelength and material selection to improve this trade-off. Although the solutions of three-dimensional plasmonic waveguides are significantly more complicated than those in the two-dimensional case solved here, the intuitive picture provided by this analysis would suggest that holes or grooves in metallic layers as opposed to metallic stripe waveguides would be the

ideal systems for subwavelength waveguides confined in two dimensions.[2,24]

ACKNOWLEDGMENTS

The authors thank Shanhui Fan for useful discussions. This work is supported in part by National Science Foundation grant Career ECS-0348800. R. Zia also acknowledges the support of a National Defense Science and Engineering Graduate Fellowship sponsored by the Office of Naval Research.

Address correspondence to Rashid Zia at zia@stanford.edu.

REFERENCES

1. W. L. Barnes, A. Dereux, and T. W. Ebbesen, "Surface plasmon subwavelength optics," Nature (London) **424**, 824–830 (2003).
2. J. Takahara, S. Yamagishi, H. Taki, A. Morimoto, and T. Kobayashi, "Guiding of a one-dimensional optical beam with nanometer diameter," Opt. Lett. **22**, 475–478 (1997).
3. M. Quinten, A. Leitner, J. R. Krenn, and F. R. Aussenegg, "Electromagnetic energy transport via linear chains of silver nanoparticles," Opt. Lett. **23**, 1331–1333 (1998).
4. M. L. Brongersma, J. W. Hartman, and H. A. Atwater, "Electromagnetic energy transfer and switching in nanoparticle chain arrays below the diffraction limit," Phys. Rev. B **62**, R16356–R16359 (2000).
5. J. C. Weeber, A. Dereux, Ch. Girard, J. R. Krenn, and J. P. Goudonnet, "Plasmon polaritons of metallic nanowires for controlling submicron propagation of light," Phys. Rev. B **60**, 9061–9068 (1999).
6. R. M. Dickson and L. A. Lyon, "Unidirectional plasmon propagation in metallic nanowires," J. Phys. Chem. B **104**, 6095–6098 (2000).
7. J. R. Krenn, B. Lamprecht, H. Ditlbacher, G. Schider, M. Salerno, A. Leitner, and F. R. Aussenegg, "Non-diffraction-limited light transport by gold nanowires," Europhys. Lett. **60**, 663–669 (2002).
8. S. A. Maier, P. G. Kik, H. A. Atwater, S. Meltzer, E. Harel, B. E. Koel, and A. A. G. Requicha, "Local detection of electromagnetic energy transport below the diffraction limit in metal nanoparticle plasmon waveguides," Nat. Mater. **2**, 229–232 (2003).
9. R. Charbonneau, P. Berini, E. Berolo, and E. Lisicka-Shrzek, "Experimental observation of plasmon–polariton waves supported by a thin metal film of finite width," Opt. Lett. **25**, 844–847 (2000).
10. D. Sarid, "Long-range surface-plasma waves on very thin metal films," Phys. Rev. Lett. **47**, 1927–1930 (1981).
11. J. J. Burke, G. I. Stegeman, and T. Tamir, "Surface-polariton-like waves guided by thin, lossy metal films," Phys. Rev. B **33**, 5186–5201 (1986).
12. F. Yang, J. R. Sambles, and G. W. Bradberry, "Long-range surface modes supported by thin films," Phys. Rev. B **44**, 5855–5872 (1991).
13. P. Berini, "Plasmon–polariton modes guided by a metal film of finite width," Opt. Lett. **24**, 1011–1013 (1999).
14. P. Berini, "Plasmon-polariton waves guided by thin lossy metal films of finite width: bound modes of asymmetric structures," Phys. Rev. B **63**, 125417 (2001).
15. E. N. Economou, "Surface plasmons in thin films," Phys. Rev. **182**, 539–554 (1969).
16. K. R. Welford and J. R. Sambles, "Coupled surface plasmons in a symmetric system," J. Mod. Opt. **35**, 1467–1483 (1988).
17. P. Tournois and V. Laude, "Negative group velocities in metal-film optical waveguides," Opt. Commun. **137**, 41–45 (1997).
18. Y. Wang, "Wavelength selection with coupled surface plasmon waves," Appl. Phys. Lett. **82**, 4385–4387 (2003).
19. H. Shin, M. F. Yanik, S. Fan, R. Zia, and M. L. Brongersma, "Omnidirectional resonance in a metal–dielectric–metal geometry," Appl. Phys. Lett. **84**, 4421–4423 (2004).
20. E. Anemogiannis and E. N. Glytsis, "Multilayer waveguides: efficient numerical analysis of general structures," J. Lightwave Technol. **10**, 1344–1351 (1992).
21. C. Chen, P. Berini, D. Feng, S. Tanev, and V. P. Tzolov, "Efficient and accurate numerical analysis of multilayer planar optical waveguides in lossy anisotropic media," Opt. Express **7**, 260–272 (2000).
22. E. Anemogiannis, E. N. Glytsis, and T. K. Gaylord, "Determination of guided and leaky modes in lossless and lossy planar multilayer optical waveguides: reflection pole method and wavevector density method," J. Lightwave Technol. **17**, 929–940 (1999).
23. E. D. Palik, *Handbook of Optical Constants and Solids* (Academic, Orlando, Fla., 1985).
24. I. V. Novikov and A. A. Maradudin, "Channel polaritons," Phys. Rev. B **66**, 035403 (2002).